Supplementary information

Synthesis, DNA and BSA binding, in vitro anti-proliferative and in vivo anti-angiogenic properties of some cobalt(III) Schiff base complexes

Yesaiyan Manojkumar[1], Subramanian Ambika[1], Rasu Arulkumar [1], Gowdhami Balakrishnan[2], Prumalsamy Balaji [2], Gobalsamy Vignesh [3], Sankaralingam Arunachalam*[1,6] Ponnambalam Venuvanalingam*[1], Ramaswamy Thirumurugan[2] Mohammad Abdulkader Akbarsha* [4,5]

Figure S1. FT-IR spectra of cobalt(III) complexes **1-4**

Figure S2. ^{1}H spectra of complexes **1- 4** in $CDCl_3$

Figure S3. ^{13}C –NMR spectra of complexes **1-4** in $CDCl_3$

Figure S4. ESI-MS spectra of complexes **1-4** in methanol

Figure S5. (A) Absorption spectra of cobalt(III) complex **1** in the absence (dotted line) and in the presence (solid line) of increasing amounts of CT-DNA. Insert: Plot of $[DNA]/(\varepsilon_a-\varepsilon_f)$ vs [DNA]. **(B)** Absorption spectra of cobalt(III) complex **2** in the absence (dotted line) and in the presence (solid line) of increasing amounts of CT-DNA. Insert: Plot of $[DNA]/(\varepsilon_a-\varepsilon_f)$ vs [DNA]. [Complex] = 5 x 10^{-5} M, [DNA] = 0- 4.6 x 10^{-4} M.

Figure S6. (A) Emission spectra of the DNA- ethidium bromide (EB) system upon the titration of complex **1**. The arrow shows the change upon the increasing complex concentration. **(B)** Emission spectra of the DNA- ethidium bromide (EB) system upon the titration of complex **2**. The arrow shows the change upon the increasing complex concentration.

Figure S7. Stern-Volmer plot of fluorescence quenching of EB bound with DNA by cobalt(III) complexes **1- 4.**

Figure S8. Circular dichroism spectra of CT-DNA (4×10^{-5} M) in the presence of increasing amounts of cobalt(III) complex **1(A)** and complex 2 **(B)**, r = [complex]/[DNA] = 0.0, 0.1, 0.5).

Figure S9. The UV-Vis absorption spectra of BSA in the absence and presence of cobalt(III) complex **1(A)** and **2 (B)** . [BSA] = 2 x 10^{-6} M; [complex] = 6 x10^{-6} M

Figure S10. A) The emission spectra of BSA in the presence of increasing amounts of cobalt(III) complex **1**. **B)**. The emission spectra of BSA in the presence of increasing amounts of cobalt(III) complex **1**. The dashed line shows the intensity in the absence of complexes. The arrow shows the fluorescence quenching upon increasing the concentration of the complexes. [BSA] = 2 x 10^{-6} M; [complex] = 0 – 6 x 10^{-6} M.

Figure S11. Stern-Volmer plot for quenching of BSA by cobalt(III) complexes **1** - **4**.

Figure S12. Plot of log[(F_0-F)/F] vs log [Q] for BSA- cobalt(III) complexes **1** - **4.**

Figure S13. Van't Hoff plots for the interaction of cobalt(III) complexes (**1 - 4**) with BSA **.**

Figure S14. 3D -Fluorescence spectra of BSA in the absence and presence of complexes **1** - **4**. [BSA] = 2 μM, [cobalt(III) complexes] = 6 μM.

Figure S15. The optimized geometries of the complexes **1- 4** at B3LYP/BS1 level of theory in gas phase. (H atoms omitted for clear visualization)

Figure S16. Docked poses of the metal complexes **1** and **2** with DNA duplex.

Figure S17. Docked poses of the metal complexes **1** and **2** into the BSA protein .

Figure S18. Inhibitory effects of *cis*platin and complexes **1- 4** and on A549 lung cancer cells treated with different concentrations for 24. All the data were expressed in Mean ± SD of two experiments with three replicate wells.

Figure S19. The graph shows data on percentage of cells that were normal or afflicted with apoptosis and necrosis in the control and experimental treatments.

Figure S20. The percentage of cells that were normal and those afflicted with apoptosis and necrosis in the control and 24 h treatment groups.

Table S1. The percentage of α–helix content of BSA in the absence and presence of cobalt(III) complexes (**1 - 4**)

Table S2. The important bond lengths (Å), bond angles (°) and dihedral angles (°) obtained from optimized geometry of the metal complexes **1-4** at B3LYP/BS1 level in gas phase.

Table S3. Theoretical IR vibrational frequencies(cm^{-1}) of complexes **1- 4**.

Table S4. Absorption maxima (λ_{cal}) from TDDFT calculations.

Table S5. The metal complexes **1- 4** interact with amino acids presence in the BSA nearby Trp 134 and binding energy corresponding to the two different binding sites.

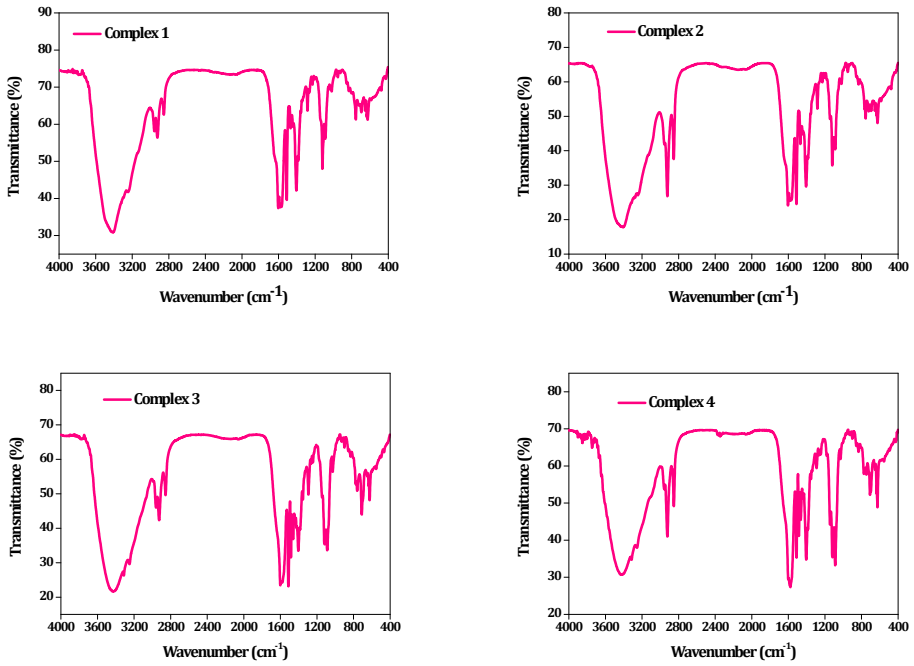

Figure S1. FT-IR spectra of cobalt(III) complexes **1-4**

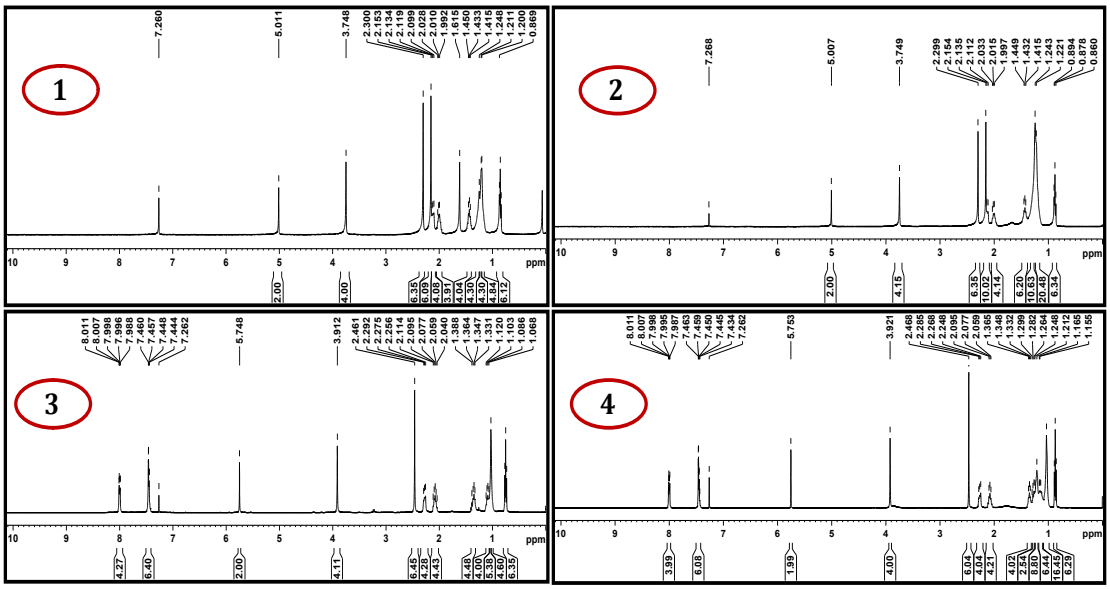

Figure S2. ^{1}H spectra of complexes **1- 4** in $CDCl_3$

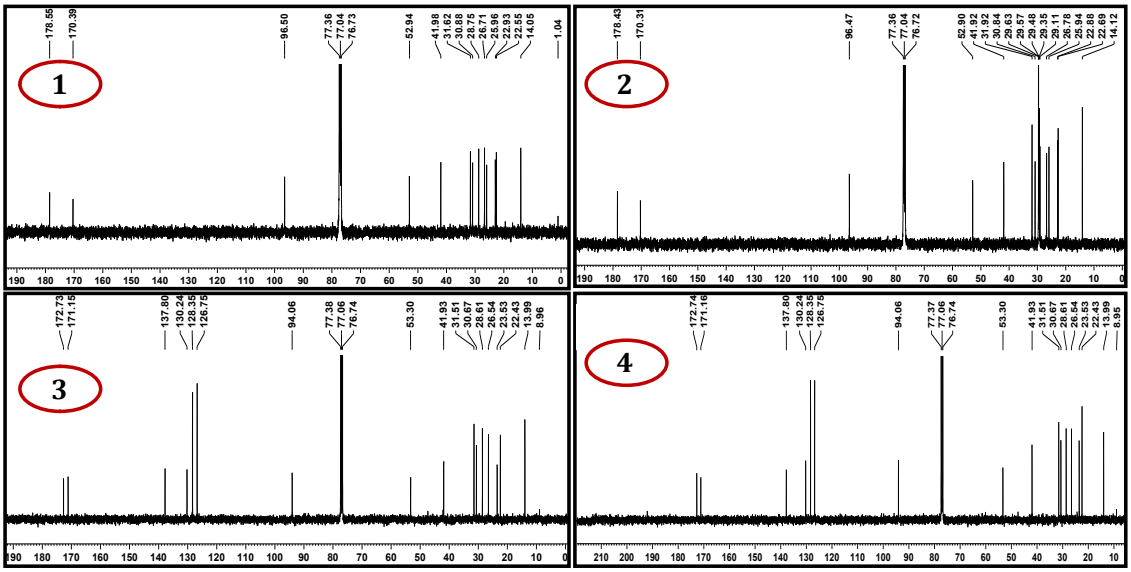

Figure S3. ^{13}C –NMR spectra of complexes **1-4** in $CDCl_3$

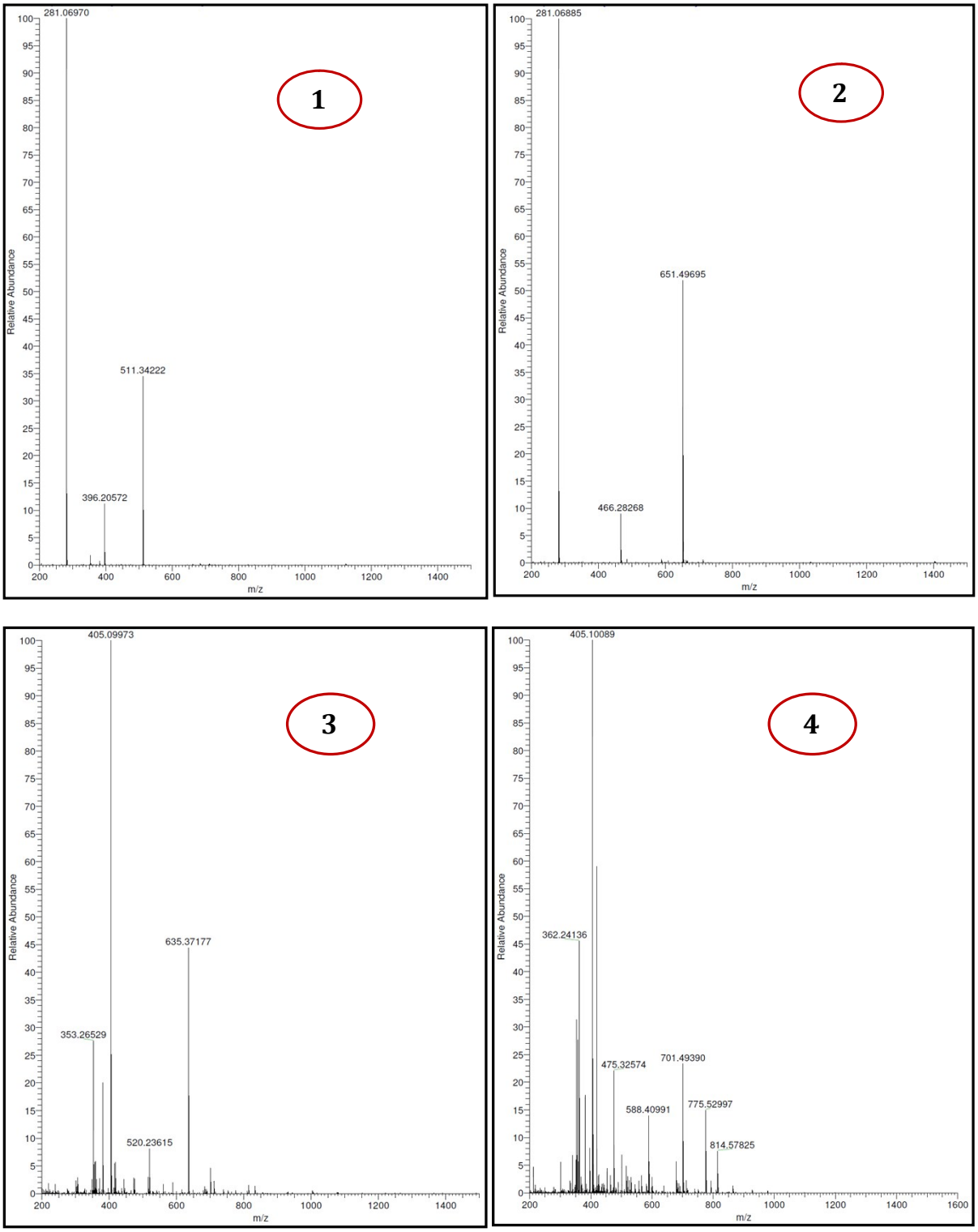

Figure S4. ESI-MS spectra of complexes **1-4** in methanol

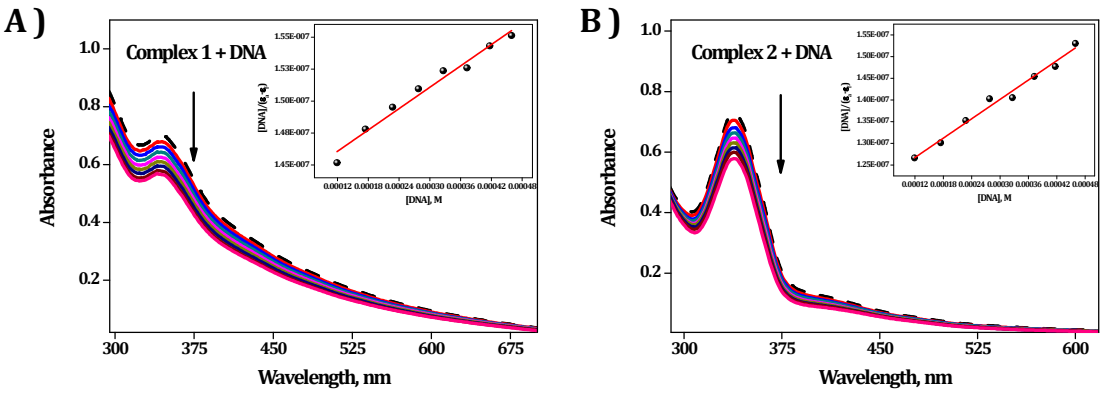

Figure S5. (A) Absorption spectra of cobalt(III) complex **1** in the absence (dotted line) and in the presence (solid line) of increasing amounts of CT-DNA. Insert: Plot of [DNA]/(ε_a-ε_f) vs [DNA]. **(B)** Absorption spectra of cobalt(III) complex **2** in the absence (dotted line) and in the presence (solid line) of increasing amounts of CT-DNA. Insert: Plot of [DNA]/(ε_a-ε_f) vs [DNA]. [Complex] = 5 x 10^{-5} M, [DNA] = 0- 4.6 x 10^{-4} M.

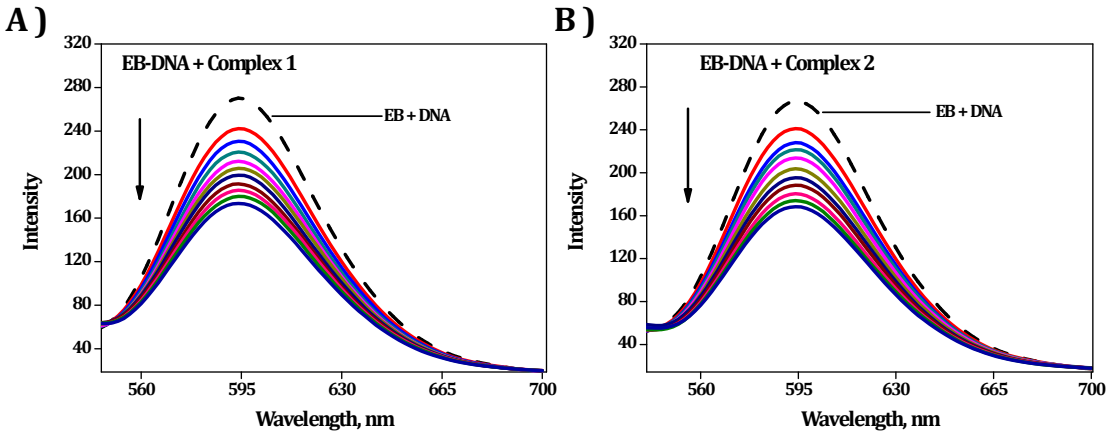

Figure S6. (A) Emission spectra of the DNA–ethidium bromide (EB) system upon the titration of complex **1**. The arrow shows the change upon the increasing complex concentration. **(B)** Emission spectra of the DNA–ethidium bromide (EB) system upon the titration of complex **2**. The arrow shows the change upon the increasing complex concentration.

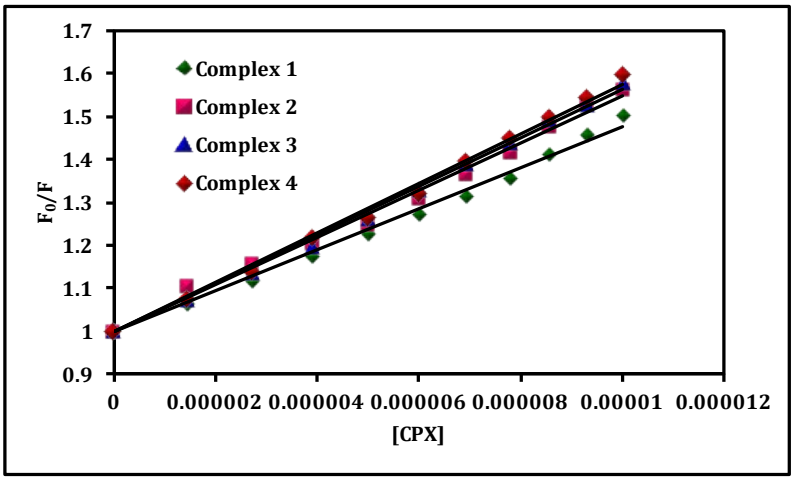

Figure S7. Stern-Volmer plot of fluorescence quenching of EB bound with DNA by cobalt(III) complexes **1-4.**

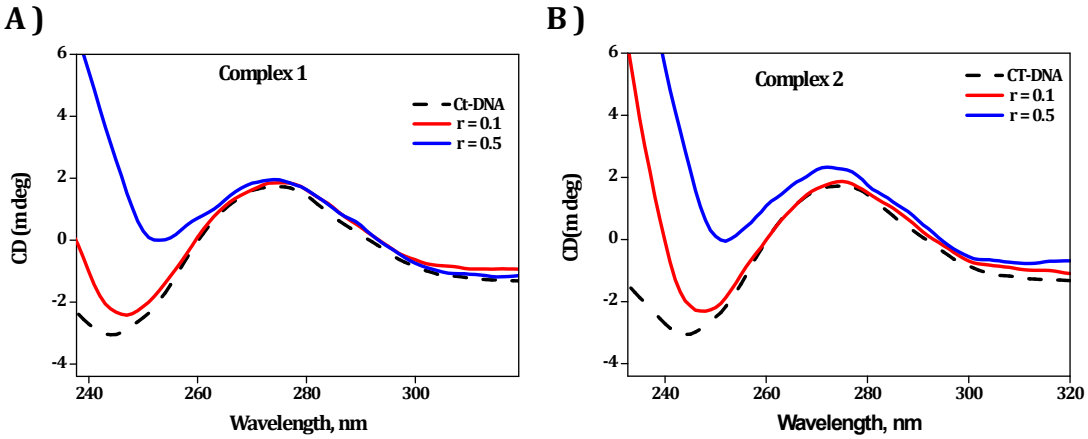

Figure S8. Circular dichroism spectra of CT-DNA (4×10^{-5} M) in the presence of increasing amounts of cobalt(III) complex **1(A)** and complex 2 **(B)**, r = [complex]/[DNA] = 0.0, 0.1, 0.5).

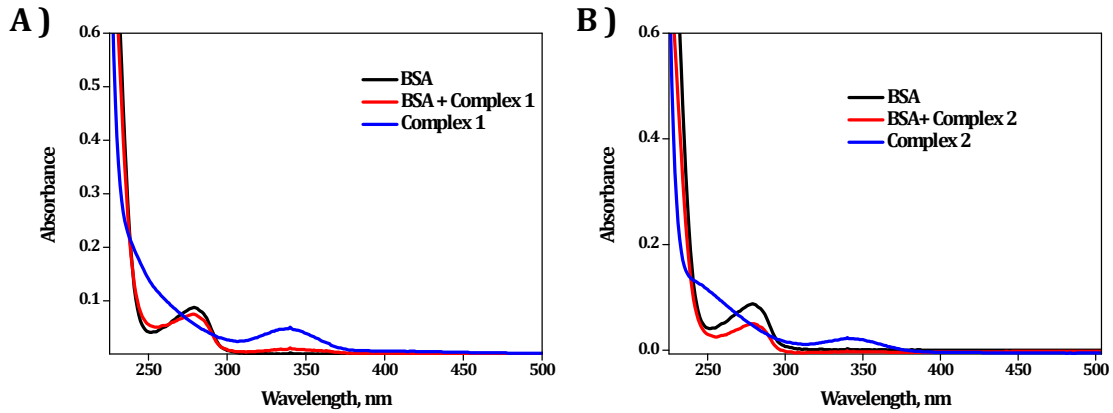

Figure S9. The UV-Vis absorption spectra of BSA in the absence and presence of cobalt(III) complex **1(A) and 2 (B)** . [BSA] = 2 x 10^{-6} M; [complex] = 6 x10^{-6} M

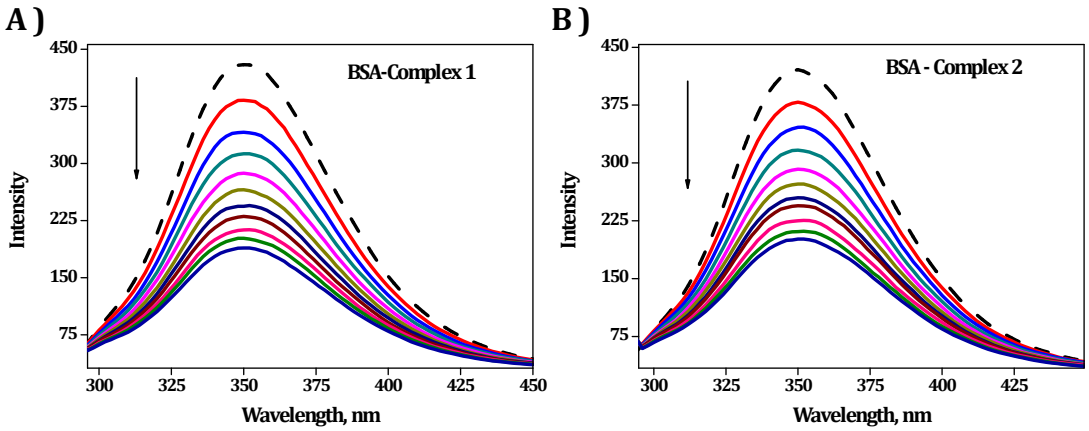

Figure S10. A) The emission spectra of BSA in the presence of increasing amounts of cobalt(III) complex **1**. **B)**. The emission spectra of BSA in the presence of increasing amounts of cobalt(III) complex **1**. The dashed line shows the intensity in the absence of complexes. The arrow shows the fluorescence quenching upon increasing the concentration of the complexes. [BSA] = 2 x 10^{-6} M; [complex] = 0 – 6 x 10^{-6} M.

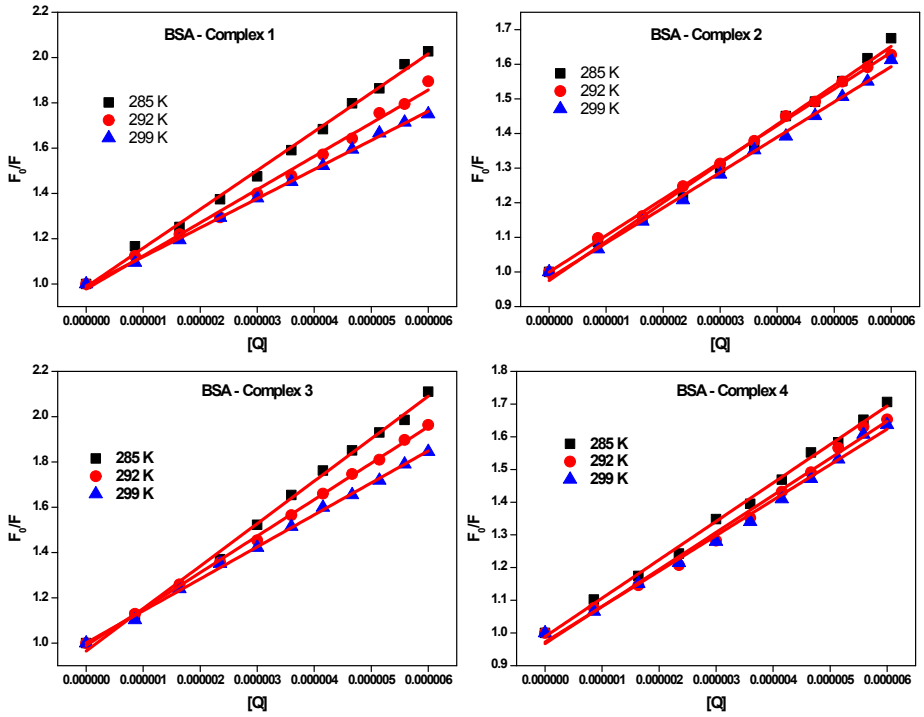

Figure S11. Stern-Volmer plot for quenching of BSA by cobalt(III) complexes **1** - **4**.

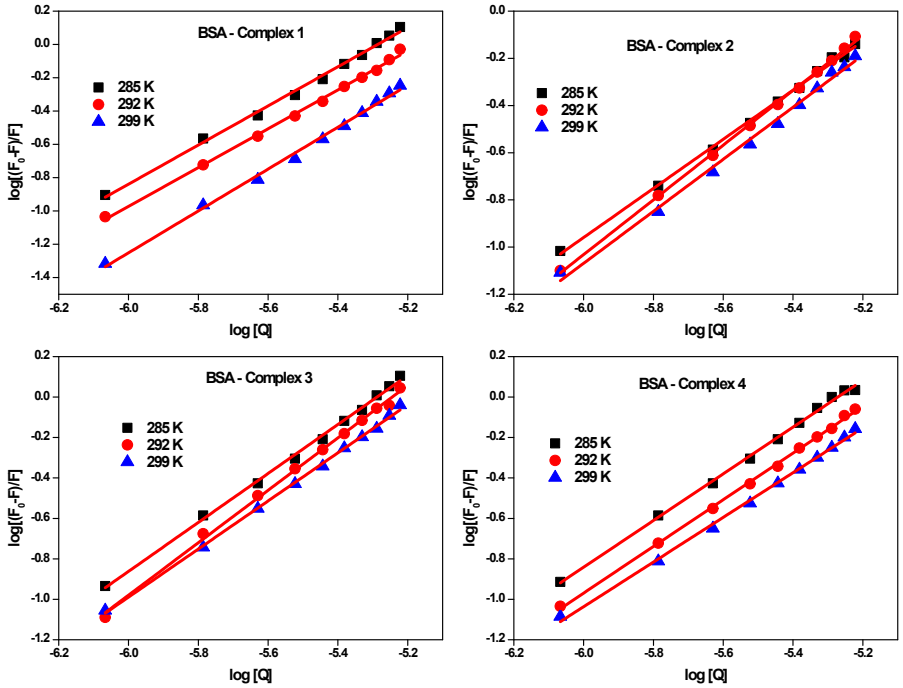

Figure S12. Plot of log[(F_0-F)/F] vs log [Q] for BSA- cobalt(III) complexes **1** - **4.**

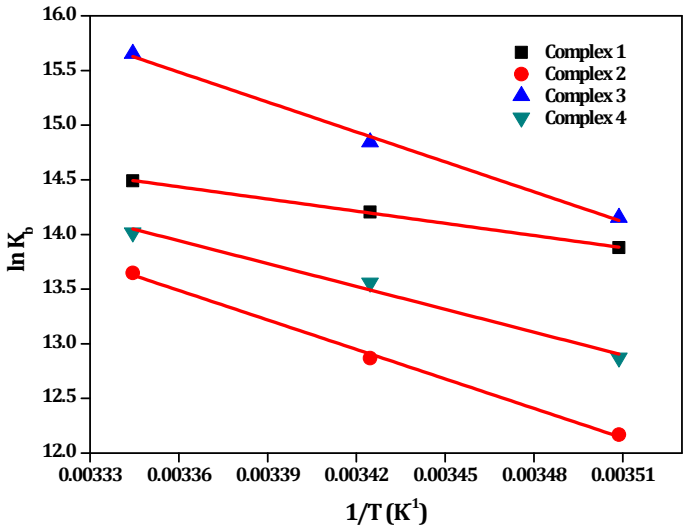

Figure S13. Van't Hoff plots for the interaction of cobalt(III) complexes (**1–4**) with BSA **.**

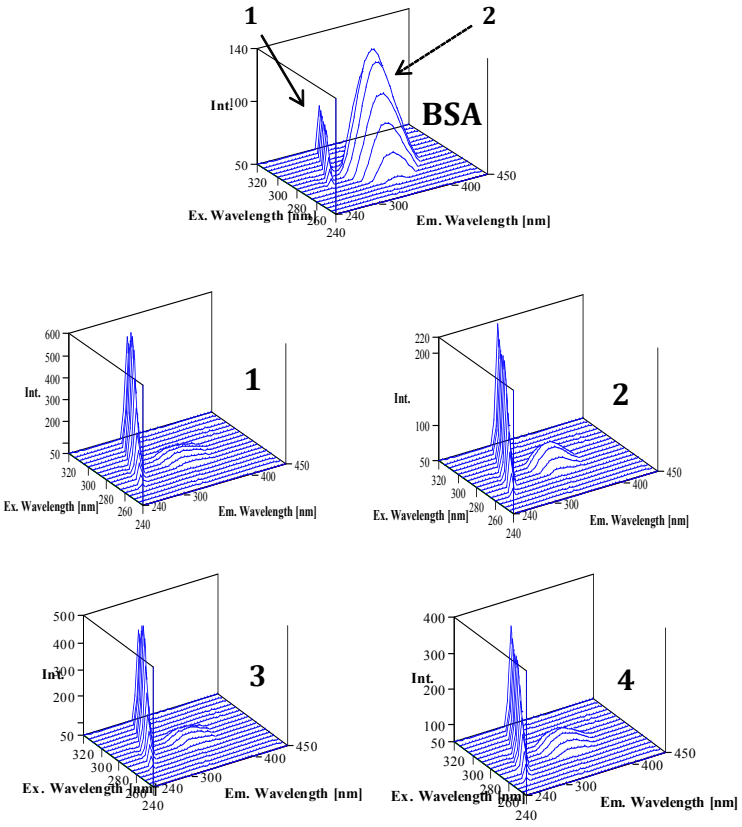

Figure S14. 3D -Fluorescence spectra of BSA in the absence and presence of complexes **1-4**. [BSA] = 2 μM, [cobalt(III) complexes] = 6 μM.

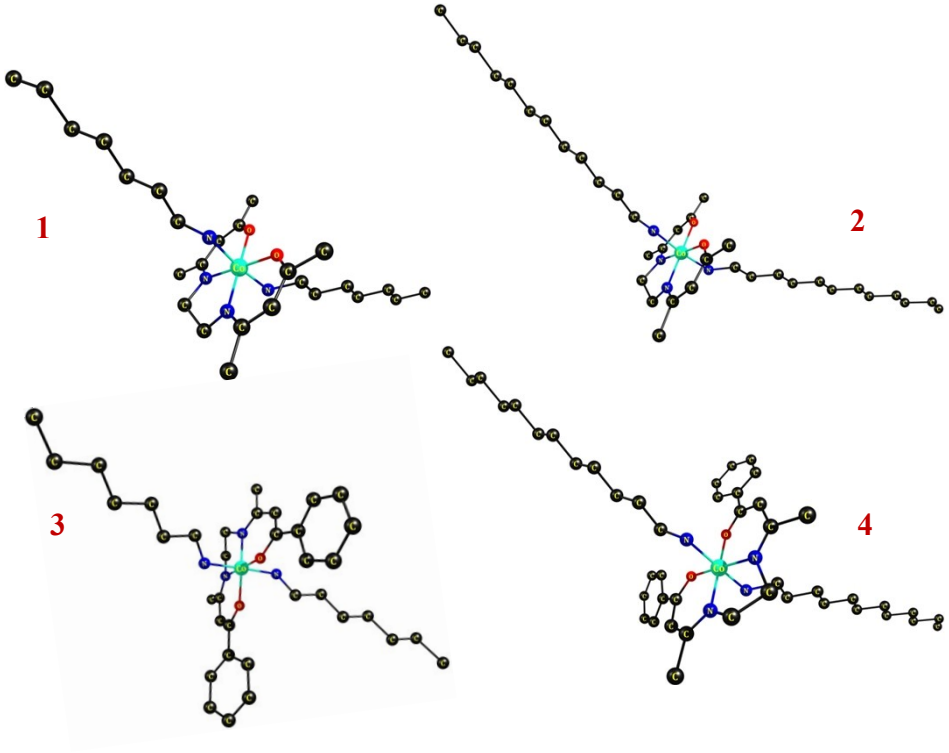

Figure S15. The optimized geometries of the complexes **1- 4** at B3LYP/BS1 level of theory in gas phase. (H atoms omitted for clear visualization)

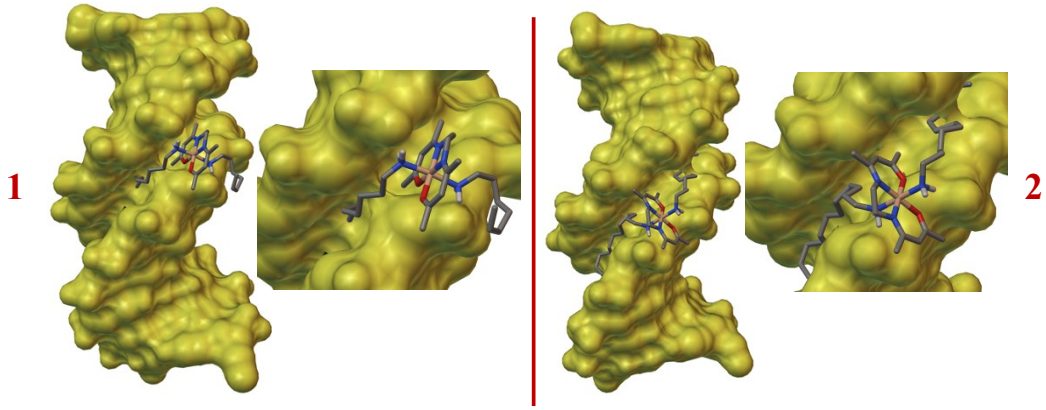

Figure S16. Docked poses of the metal complexes **1** and **2** with DNA duplex.

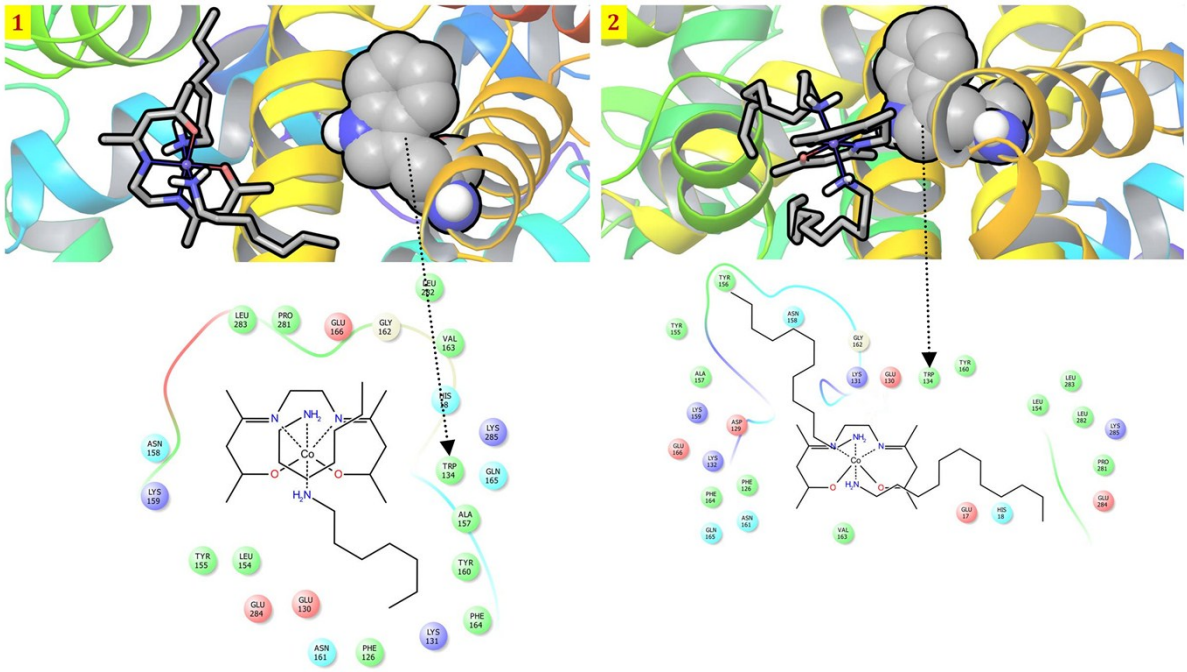

Figure S17. Docked poses of the metal complexes **1** and **2** into the BSA protein.

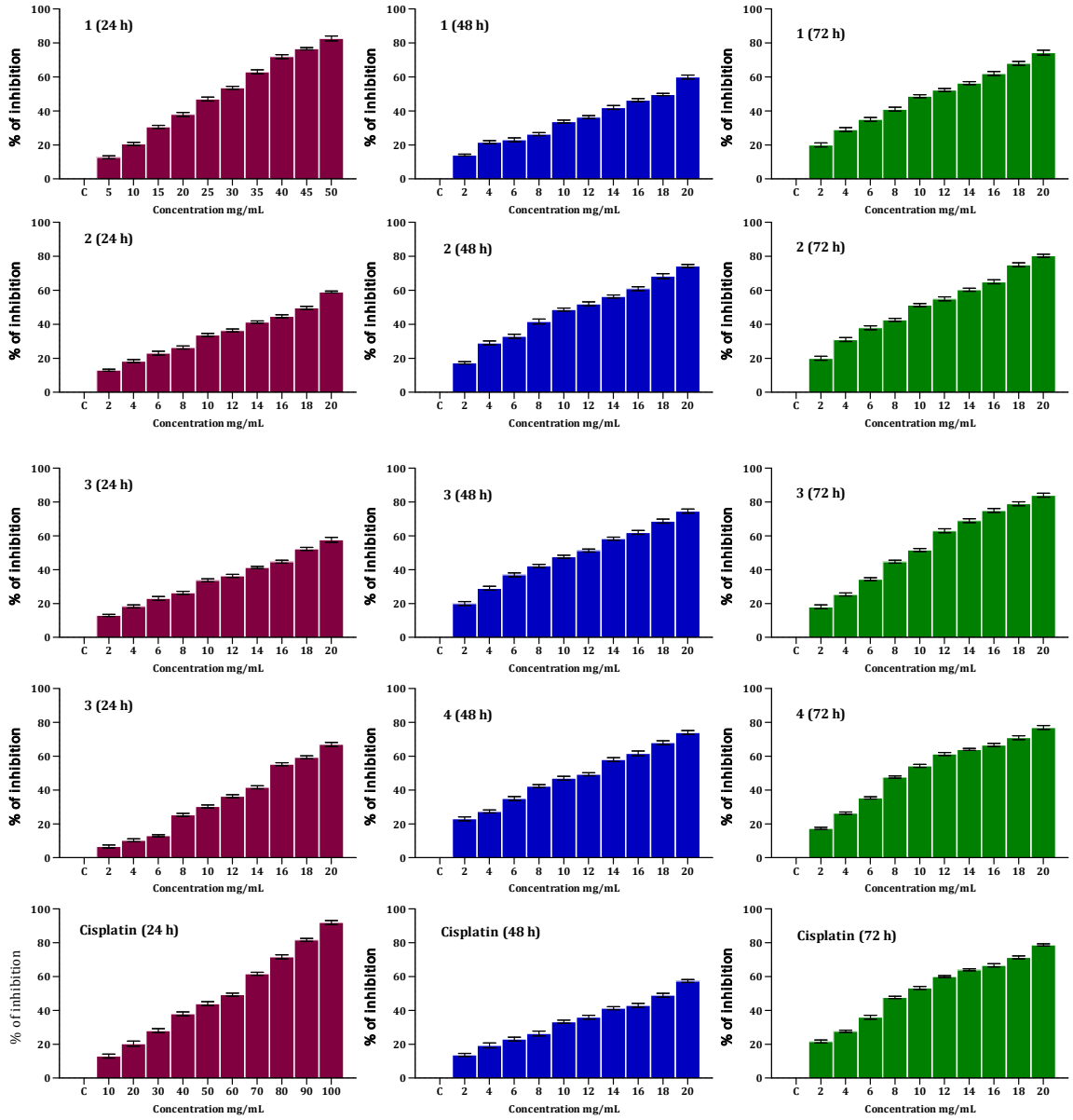

Figure S18. Inhibitory effects of *cis*-platin and complexes **1- 4** and on A549 lung cancer cells treated with different concentrations for 24, 48 and 72 h. Data were obtained in triplicates each, and used to calculate the means and the standard deviations.

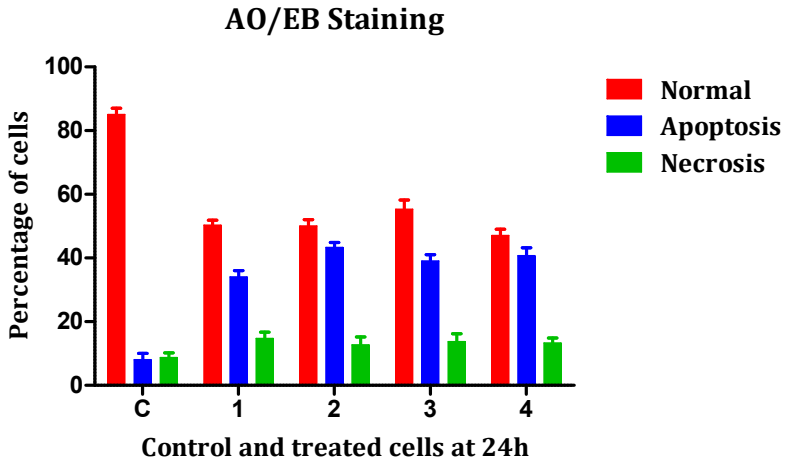

Figure S19. The graph shows data on percentage of cells that were normal or afflicted with apoptosis and necrosis in the control and experimental treatments.

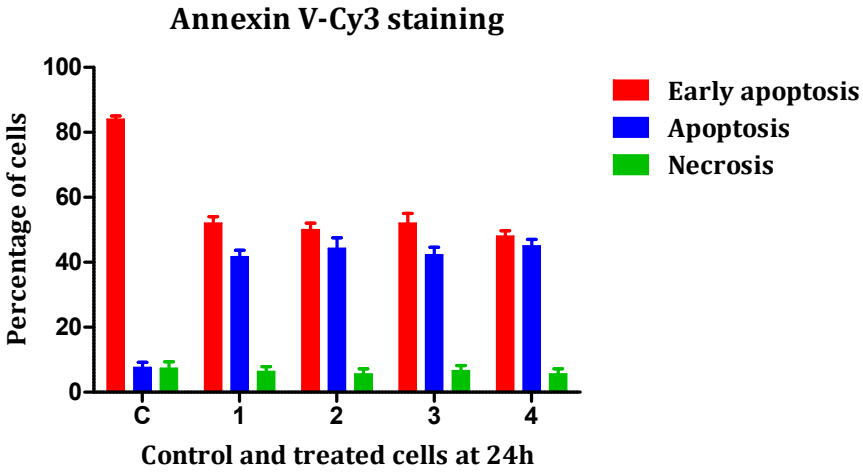

Figure S20. The percentage of cells that were normal and those afflicted with apoptosis and necrosis in the control and 24 h treatment groups.

Table S1. The percentage of α–helix content of BSA in the absence and presence of cobalt(III) complexes (1-4)

Complexes	α–helix (%)
BSA	69.50
1	55.54
2	64.28
3	52.78
4	62.78

Table S2 The important bond lengths (Å), bond angles (°) and dihedral angles (°) obtained from optimized geometry of the metal complexes **1-4** at B3LYP/BS1 level in gas phase.

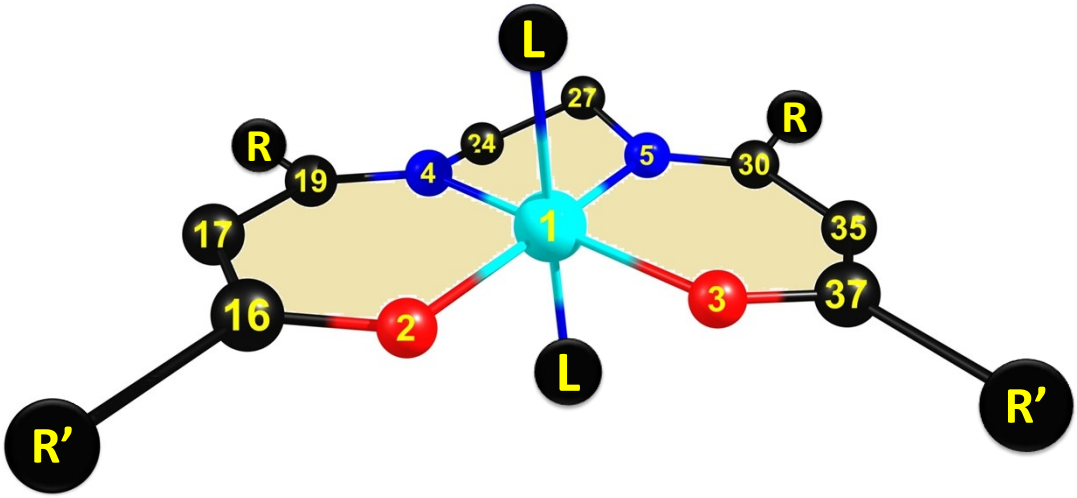

Bond Parameters	Complex 1	Complex 2	Complex 3	Complex 4
		Bond Lengths (Å)		
Co1-O2	1.914	1.913	1.914	1.915
Co1-O3	1.909	1.909	1.908	1.909
Co1-N4	1.937	1.936	1.933	1.933
Co1-N5	1.934	1.932	1.923	1.925
Co1-N6	2.004	2.005	2.006	2.005
Co1-N9	2.009	2.008	2.006	2.009
		Bond Angles (°)		
O2-Co1-O3	85.6	85.5	86.3	85.9
O2-Co1-N4	94.2	94.3	94.1	94.2
N4-Co1-N5	85.6	85.7	85.7	85.7
N6-Co1-N9	173.9	174.5	175.1	174.5
		Dihedral Angles (°)		
C37-O3-Co1-N4	-137.8	122.0	-30.98	-78.9
O3-Co1-O2-C16	171.3	175.1	179.6	176.3

Table S3. Theoretical IR vibrational frequencies(cm^{-1}) of complexes 1- 4.

Band	Complex 1	Complex 2	Complex 3	Complex 4
γ **C-N**	1572	1573	1591	1591
γ **C-O**	1233	1233	1241	1243
γ **C-H(s)**	2922	2925	2921	2921
γ **N-H**	3407	3412	3413	3413

Table S4. Absorption maxima (λ_{cal}) from TDDFT calculations.

Complex	States	Major contribution	Oscillator Strength (f)	E (eV)	λ_{cal}(nm)
1	$S_0 \rightarrow S_9$	HOMO→LUMO+2(70%)	0.0131	3.86	321.5
	$S_0 \rightarrow S_{10}$	HOMO→LUMO+3(64%)	0.0630	3.94	314.7
2	$S_0 \rightarrow S_9$	HOMO→LUMO+2(70%)	0.0126	3.85	321.8
	$S_0 \rightarrow S_{10}$	HOMO→LUMO+3(63%)	0.0616	3.94	314.5
3	$S_0 \rightarrow S_7$	HOMO→LUMO+1(63%)	0.0363	3.33	372.5
	$S_0 \rightarrow S_8$	HOMO→LUMO+2(36%)	0.1078	3.43	361.9
4	$S_0 \rightarrow S_7$	HOMO→LUMO+1(68%)	0.0428	3.33	372.1
	$S_0 \rightarrow S_8$	HOMO→LUMO+2(42%)	0.1179	3.42	362.8

Table S5. The metal complexes **1-4** interact with amino acids presence in the BSA nearby Trp 134 and binding energy corresponding to the two different binding sites.

Complexes	Interacting amino acids in BSA binding site (Trp 134)	Binding Energy in kcal/mol	
		Trp134	Trp213
1	TRP134, LYS285, GLN165, ALA157, TYR160, PHE164, LYS131, PHE126, ASN161, GLU130, GLU284, LEU154, TYR155, LYS159, ANS158, LEU283, PRO281, GLU166, GLY162, LEU282, VAL163, HIS18	-5.60	-4.82
2	TRP134, TYR160, LEU154, LEU283, LEU 282, LYS285, PRO281, GLU284, HIS18, GLU17, VAL163, ASN161, GLN165, PHE164, PHE126, LYS132, GLU166, ASP129, LYS159, ALA157, TYR155, TYR156, ASN158, GLY162, LYS131, GLU130	-4.96	-4.24
3	TRP134, ALA157, ASN161, LYS159, ASN158, VAL163, GLY162, GLN165, GLU130,GLU166, PHE126, PHE164, LYS280, GLU284, PRO281, LEU282, LEU283, HIS18, LEU154, TYR155, LYS131, TYR160	-6.70	-4.53
4	TRP134, LYS131, GLY135, GLY21, LEU138, LEU24, GLU17, VAL23, HIS18, VAL43, LYS20, LEU22, PHE36, HIS39, VAL40, ASN44, ASN158, LEU283, TYR160, ALA157, LYS159, GLY162, GLN165, LYS132, ASN161, PHE126, PHE164, ASP129, GLU130, GLU16	-5.14	-3.79